Asociación Argentina
de Mecánica Computacional

Mecánica Computacional Vol XXXV, págs. 39-47 (artículo completo)
Martín I. Idiart, Ana E. Scarabino y Mario A. Storti (Eds.)
La Plata, 7-10 Noviembre 2017

ABSORBING BOUNDARY CONDITIONS FOR 3D ANISOTROPIC MEDIA

Patricia M. Gauzellino[a,b] **and Juan E. Santos**[b,c,d]

[a]*Depto. de Geofísica Aplicada, Universidad Nacional de La Plata, Paseo del Bosque s/No, 1900 La Plata, Argentina, gauze@fcaglp.unlp.edu.ar*

[b]*Facultad de Ingeniería, Universidad Nacional de La Plata, Calle 1 y 47, 1900 La Plata, Argentina*

[c]*Facultad de Ingeniería, Instituto del Gas y del Petróleo, Universidad de Buenos Aires, Av. Las Heras 2214 Piso 3 C1127AAR C.A.B.A., Argentina*

[d]*Department of Mathematics, Purdue University, Indiana, USA, santos@math.purdue.edu*

Keywords: Boundary conditions, anisotropy, finite elements, mechanical waves.

Abstract. Seismic methods of subsurface exploration are based on mechanical wave propagation and the numerical modeling of these phenomena is a worthy tool that can be applied as a complement. Since small regions of Earth's crust are studied, it is necessary to consider absorbing boundary conditions for solving the wave equations efficiently. Therefore, this work presents a derivation of low-order absorbing boundary conditions at the artificial boundaries of the computational domain with the purpose of minimizing spurious reflections. Laboring on a surface S, which separates disturbed and undisturbed regions of the domain, the equations for the absorbing boundary conditons are derived from kinematic conditions, considering continuity of the displacements across S and dynamic conditions, using momentum equations of the wave fronts arriving normally to S and expressions for the strain energy density along S. The arguments to obtain non-reflecting artificial boundaries are carried out for the more general case, through the generalized Hooke's law. In this way, an isotropic medium is included in this derivation. The performance of these absorbing boundary conditions is illustrated for different models of effective anisotropy -vertically and tilted transversely isotropic media- and, obviously, for isotropic media. The numerical simulations use these absorbing boundary conditions to propagate waves in anisotropic media using an iterative domain decomposition finite element procedure that is implemented in machines with parallel architecture.

1 INTRODUCCIÓN

The numerical simulation of the seismic wave propagation is a valuable tool for understanding geophysical phenomena and interpreting the field data, particularly in hydrocarbon exploration and production. The regions of study are small zones of the Earth's crust where the computational domain has to behave as a unbounded area. In this scenario, it is important to solve the wave equation with absorbing boundary conditions (ABC) in isotropic and anisotropic media.

Classical procedure for the implementation of ABC is proposed by Engquist and Majda (1977). However,they present problems in some anisotropic media. Perfectly Matched Layer (PML) is implemented by Bérenger (1994) for electromagnetic waves and can be seen its efficiency for elastic waves in Collino and Tsogka (2001). It should be noted that when using PML the wave equation must be written as a first-order system in velocity and stress. Komatitsch and Tromp (2003) reformulate the classical PML condition and solve the elastic wave equation written as a second-order system in displacement and using finite element technique.

The idea of using the information of the wavefronts in anisotropic elastic media has been presented by Bécache et al. (2010) and Savadatti and Gudatti (2012). Also, Boillot et al. (2015) use the information of wave-front sets following the slowness curves (2-D) or slowness surfaces (3-D) in tilted transverse isotropic media, deriving low-order absorbing boundary conditions.

In this work, following the idea of Lovera and Santos (1988), we present a development to obtain low-order absorbing boundary conditions in the artificial borders of the model that limit the computational area. These conditions can be applied to solve elastic or viscoelastic wave propagation written as a single second-order equation and in media with any type of anisotropy. We use an iterative domain decomposition finite element procedure that is implemented in machines with parallel architecture imperative for three-dimensional problems.

2 FORMULATION OF THE ANISOTROPIC PROBLEM

Let Ω be an open bounded domain, $\Omega \subset \mathbb{R}^3$ with artificial boundaries Γ. Let $\mathbf{u}(\mathbf{x},t) = (u_1(\mathbf{x},t), u_2(\mathbf{x},t), u_3(\mathbf{x},t))$ be the displacement and let $\mathbf{f}$ be an external source. Wave propagation phenomena in the time-space domain are governed by the equation

$$\rho(\mathbf{x})\frac{\partial^2 \mathbf{u}(\mathbf{x},t)}{\partial t^2} - \nabla \cdot \tau(\mathbf{u}(\mathbf{x},t)) = f, \quad \mathbf{x} \in \Omega, \quad t \geq 0, \tag{1}$$

where ρ is the density and τ is the stress tensor.

We choose to work in the space-frequency domain because it is the natural domain for dealing with attenuation and dispersion phenomena. For example, the presence of fractures with some preferential orientation induces this kind of effects.

Taking Fourier transform in the time domain, the equation (1) becomes

$$-\rho(\mathbf{x})\omega^2 \hat{\mathbf{u}}(\mathbf{x},\omega) - \nabla \cdot \tau(\mathbf{u}(\mathbf{x},\omega)) = \mathbf{f}, \quad \mathbf{x} \in \Omega \tag{2}$$

The stress tensor, τ, is related to the strain tensor, ε, by the Hooke's law

$$\tau_{ij}(\mathbf{u},\omega) = \sum_{k,l} p_{ijkl}(\mathbf{x},\omega)\varepsilon_{kl}(\mathbf{u}), \quad (i,j,k,l = 1,2,3), \tag{3}$$

being $\mathbf{p}$ the fourth-rank stiffness tensor with symmetry properties that are manifested in the scalar strain-energy density given by (see Landau and Lifshitz (1959); Aki and Richards (1980))

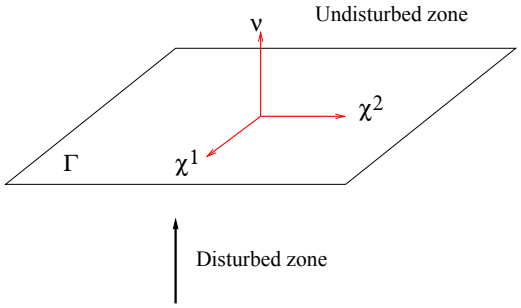

Figure 1: Surface Γ moving with velocity and separating disturbed zone of other undisturbed.

$$\mathcal{W} = \frac{1}{2}\tau_{ij}\varepsilon_{ij} = \frac{1}{2}p_{ijkl}\varepsilon_{ij}\varepsilon_{kl} \tag{4}$$

To solve the differential equation(2) it is necessary to establish boundary conditions.

3 ABSORBING BOUNDARY CONDITIONS

The ABC for the artificial boundary Γ is given by

$$\begin{aligned}(-\tau(\mathbf{u}(x,\omega))\nu\cdot\nu, -\tau(\mathbf{u}(x,\omega))\nu\cdot\chi^1, -\tau(\mathbf{u}(x,\omega))\nu\cdot\chi^2) \\ = \mathrm{i}\omega\mathcal{B}_p(\mathbf{u}(x,\omega)\cdot\nu, \mathbf{u}(x,\omega)\cdot\chi^1, \mathbf{u}(x,\omega)\cdot\chi^2), \quad x\in\Gamma.\end{aligned} \tag{5}$$

Let's suppose that a surface Γ moves with velocity c and separates one disturbed zone of another undisturbed as shown in Figure 1. Let $\mathbf{u}^c$ be the displacement vector, then $\mathbf{u}^c \neq 0$ in the disturbed region and $\mathbf{u}^c \equiv 0$ in the undisturbed region. On the surface, the following conditions must be satisfied.

3.1 Kinematic conditions

The displacement is continuous across the surface so that $\mathbf{u}^c(\mathbf{x},t) \equiv 0$ on Γ. Therefore,

$$\frac{\partial u_i^c}{\partial x} = \nabla u_i^c \cdot \chi = 0$$

and ν is normal to Γ. So that

$$\nabla u_i^c = \gamma\nu \ , \ \nabla u_i^c \cdot \nu = \gamma\nu\cdot\nu = \gamma \quad \text{and} \quad \gamma = \frac{\partial u_i^c}{\partial \nu}.$$

Hence

$$\left(\frac{\partial u_i^c}{\partial x_1}, \frac{\partial u_i^c}{\partial x_2}, \frac{\partial u_i^c}{\partial x_3}\right) = \frac{\partial u_i^c}{\partial \nu}\cdot(\nu_1,\nu_2,\nu_3)$$

and

$$\frac{\partial u_i^c}{\partial \nu} = \frac{\dfrac{\partial u_i^c}{\partial x_1}}{\nu_1} = \frac{\dfrac{\partial u_i^c}{\partial x_2}}{\nu_2} = \frac{\dfrac{\partial u_i^c}{\partial x_3}}{\nu_3}. \tag{6}$$

Note that also must be met

$$\begin{aligned}u_i^c(x_1 + c\delta t\nu_1, x_2 + c\delta t\nu_2, x_3 + c\delta t\nu_3, t+\delta t) \\ = u_i^c(x_1,x_2,x_3,t) + \frac{\partial u_i^c}{\partial x_j}\nu_j c\delta t + \tfrac{\partial u_i^c}{\partial t}\delta t = 0.\end{aligned}$$

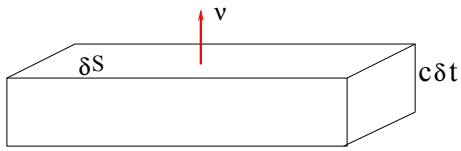

Figure 2: The volume of the prismatic element with unit normal ν and area element δS is given by $\delta\Gamma c\delta t$.

Thus, on the surface

$$c\frac{\partial u_i^c}{\partial \nu} + \frac{\partial u_i^c}{\partial t} = \frac{\partial u_i^c}{\partial t} + c\nabla u_i^c \cdot \nu = 0 \quad \text{on} \quad \Gamma. \tag{7}$$

From (6) and (7) we obtain the expressions

$$\frac{\frac{\partial u_i^c}{\partial x_1}}{\nu_1} = -\frac{1}{c}\frac{\partial u_i^c}{\partial t} \quad , \quad \frac{\frac{\partial u_i^c}{\partial x_2}}{\nu_2} = -\frac{1}{c}\frac{\partial u_i^c}{\partial t} \quad , \quad \frac{\frac{\partial u_i^c}{\partial x_3}}{\nu_3} = -\frac{1}{c}\frac{\partial u_i^c}{\partial t}. \tag{8}$$

3.2 Dynamic conditions

The dynamic conditions are obtained by applying the law of momentum conservation. Figure 2 shows a prismatic element whose volume is $V_s = \delta\Gamma c\delta t$ and its unit normal is ν. According to the expression of momentum written by Loeve (1944)

$$\frac{d}{dt}\int_{V_s} \rho \dot{u}_i^c dV_s = \int_{\delta S} F_{s,i} d\Gamma$$

As $u_i^c = 0$ on $\Gamma \equiv S$

$$\begin{aligned}\int_t^{t+\delta t}\left(\tfrac{d}{dt}\int_{V_s}\rho\dot{u}_i^c dV_s\right)dt &= \rho\left(\dot{u}_i^c(x_1,x_2,x_3,t+\delta t) - \dot{u}_i^c(x_1,x_2,x_3,t)\right)V_s \\ &= \rho\dot{u}_i^c(x_1,x_2,x_3,t+\delta t)c\delta t\delta\Gamma \\ &= \int_t^{t+\delta t}\left(\int_{\delta S} F_{s,i}d\Gamma\right)dt.\end{aligned}$$

Then, the change of momentum is equal to the integral of time of the traction acting through the surface Γ. The traction is

$$F_{s,i} = -\tau_{i,j}\nu_j$$

where $\tau_{i,j}$ is given by (3).

Therefore,

$$\rho\dot{u}_i^c(x_1,x_2,x_3,t+\delta t)c\delta t\delta\Gamma = \int_t^{t+\delta t}\int_{\delta S}(-\tau_{i,j}\nu_j)d\Gamma = (-\tau_{i,j}\nu_j)\delta t\delta\Gamma.$$

For δt and $\delta\Gamma$ tending to zero,

$$\rho c\dot{u}_i^c = -\tau_{i,j}\nu_j = \frac{\partial \mathcal{W}}{\partial \epsilon_{i,j}}\nu_j$$

In vector notation the previous equation on Γ is

$$\rho c\dot{\mathbf{u}}^c = -\tau\nu = -F_s.$$

Projecting on the local coordinate system, we obtain

$$\rho c\dot{\mathbf{u}}^c\cdot\nu = -\tau\nu\cdot\nu, \quad \rho c\dot{\mathbf{u}}^c\cdot\chi^1 = -\tau\nu\cdot\chi^1, \quad \rho c\dot{\mathbf{u}}^c\cdot\chi^2 = -\tau\nu\cdot\chi^2 \tag{9}$$

and we define $\mathbf{v}^c = (v_1^c, v_2^c, v_3^c)^t$ being

$$v_1^c = \frac{1}{c}\dot{\mathbf{u}}^c \cdot \nu = \frac{1}{c}\dot{u}_i^c \nu_i, \quad v_2^c = \frac{1}{c}\dot{\mathbf{u}}^c \cdot \chi^1 = \frac{1}{c}\dot{u}_i^c \chi_i^1, \quad v_3^c = \frac{1}{c}\dot{\mathbf{u}}^c \cdot \chi^2 = \frac{1}{c}\dot{u}_i^c \chi_i^2. \tag{10}$$

The equations (9) in function of the new variables become

$$c^2 \rho v_1^c = -\tau\nu \cdot \nu, \qquad c^2 \rho v_2^c = -\tau\nu \cdot \chi^1, \qquad c^2 \rho v_3^c = -\tau\nu \cdot \chi^2. \tag{11}$$

To also write the equation (11) as a function of v_1^c, v_2^c y v_3^c. On Γ the strains can be expressed

$$\varepsilon_{ij}(\mathbf{u}^c) = \frac{1}{2}\left(\frac{\partial u_i^c}{\partial x_j} + \frac{\partial u_j^c}{\partial x_i}\right)$$

and using (8) we obtain

$$\varepsilon_{ij}(\mathbf{u}^c) = -\frac{1}{2}\left(\nu_j \frac{1}{c}\dot{u}_i^c + \nu_i \frac{1}{c}\dot{u}_j^c\right). \tag{12}$$

3.3 Anisotropic form of the ABC

The four subscripts of the stiffness tensor are reduced to two following Voigt's notation and the stresses and strains are written as

$$\begin{pmatrix} \tau_{11} \\ \tau_{22} \\ \tau_{33} \\ \tau_{23} \\ \tau_{13} \\ \tau_{12} \end{pmatrix} = \begin{pmatrix} p_{11} & p_{12} & p_{13} & 0 & 0 & 0 \\ p_{21} & p_{22} & p_{23} & 0 & 0 & 0 \\ p_{31} & p_{32} & p_{33} & 0 & 0 & 0 \\ 0 & 0 & 0 & p_{44} & 0 & 0 \\ 0 & 0 & 0 & 0 & p_{55} & 0 \\ 0 & 0 & 0 & 0 & 0 & p_{66} \end{pmatrix} \begin{pmatrix} \varepsilon_{11} \\ \varepsilon_{22} \\ \varepsilon_{33} \\ 2\varepsilon_{23} \\ 2\varepsilon_{13} \\ 2\varepsilon_{12} \end{pmatrix}.$$

There are nine independent constants for the more general orthorhombic symmetry.

Then, τ_{ij} can be expressed depending on $\varepsilon_{ij}(\mathbf{u}^c)$, for instance,

$$\tau_{23} = 2p_{44}\varepsilon_{23} = 2p_{44}\left(\begin{array}{c} \cdots\cdots \\ -\frac{1}{2}\left(\nu_3 \frac{1}{c}\dot{u}_2^c + \nu_2 \frac{1}{c}\dot{u}_3^c\right) \\ \cdots\cdots \end{array}\right)$$

Now, let's look at a side of the cube whose local coordinate axes are $\nu = (0,0,1)$, $\chi^1 = (1,0,0)$ and $\chi^2 = (0,1,0)$. The equation (10) determines the components

$$v_1^c = \frac{1}{c}\dot{u}_i^c \nu_i = \frac{1}{c}\dot{u}_3^c, \quad v_2^c = \frac{1}{c}\dot{u}_i^c \chi_i^1 = \frac{1}{c}\dot{u}_1^c, \quad v_3^c = \frac{1}{c}\dot{u}_i^c \chi_i^2 = \frac{1}{c}\dot{u}_2^c.$$

The equation (12) determines the strains

$$\varepsilon_{11}(\mathbf{u}^c) = 0, \quad \varepsilon_{22}(\mathbf{u}^c) = 0, \quad \varepsilon_{33}(\mathbf{u}^c) = -\frac{1}{c}\dot{u}_3^c = -v_1^c,$$

$$\varepsilon_{23}(\mathbf{u}^c) = -\frac{1}{2}\frac{1}{c}\dot{u}_2^c = -\frac{1}{2}v_3^c, \quad \varepsilon_{13}(\mathbf{u}^c) = -\frac{1}{2}\frac{1}{c}\dot{u}_1^c = -\frac{1}{2}v_2^c, \quad \varepsilon_{12}(\mathbf{u}^c) = 0.$$

In this case, the stress-strain relations are

$$\begin{aligned}
\tau_{11}(\mathbf{u}^c) &= p_{13}\left(-\tfrac{1}{c}\dot{u}_3^c\right) = p_{13}(-v_1^c),\\
\tau_{22}(\mathbf{u}^c) &= p_{23}\left(-\tfrac{1}{c}\dot{u}_3^c\right) = p_{23}(-v_1^c),\\
\tau_{33}(\mathbf{u}^c) &= p_{33}\left(-\tfrac{1}{c}\dot{u}_3^c\right) = p_{33}(-v_1^c),\\
\tau_{23}(\mathbf{u}^c) &= p_{44}\left(-\tfrac{1}{c}\dot{u}_2^c\right) = p_{44}(-v_3^c),\\
\tau_{13}(\mathbf{u}^c) &= p_{55}\left(-\tfrac{1}{c}\dot{u}_1^c\right) = p_{55}(-v_2^c),\\
\tau_{12}(\mathbf{u}^c) &= 0.
\end{aligned}$$

Analyzing the projections on Γ we get

$$\begin{aligned}
-\tau\nu\cdot\nu &= -\tau_{ij}\nu_i\nu_j = -\tau_{33} = p_{33}v_1^c,\\
-\tau\nu\cdot\chi^{=} &- \tau_{ij}\nu_i\chi_j^1 = -\tau_{13} = p_{55}v_2^c,\\
-\tau\nu\cdot\chi^2 &= -\tau_{ij}\nu_i\chi_j^2 = -\tau_{23} = p_{44}v_3^c.
\end{aligned}$$

Taking into account the expression (4) on the surface

$$2\mathcal{W} = \tau_{ij}\varepsilon_{ij} = 2\tau_{13}\varepsilon_{13} + 2\tau_{23}\varepsilon_{23} + \tau_{33}\varepsilon_{33},$$

and consequently,

$$2\mathcal{W} \equiv 2\Pi(\mathbf{v}^c) = p_{33}(v_1^c)^2 + p_{55}(v_2^c)^2 + p_{44}()^2.$$

The last expression can be written as $\frac{1}{2}\mathbf{v}^c\mathcal{E}(\mathbf{v}^c)^t$, i.e.,

$$\Pi(\mathbf{v}^c) = \frac{1}{2}\begin{pmatrix} v_1^c & v_2^c & v_3^c \end{pmatrix}\begin{pmatrix} p_{33} & 0 & 0\\ 0 & p_{55} & 0\\ 0 & 0 & p_{44}\end{pmatrix}\begin{pmatrix} v_1^c\\ v_2^c\\ v_3^c\end{pmatrix}.$$

In addition,

$$\rho c^2 v_1^c = -\frac{\partial\Pi}{\partial v_1^c} = -p_{33}v_1^c, \quad \rho c^2 v_2^c = -\frac{\partial\Pi}{\partial v_2^c} = -p_{55}v_2^c, \quad \rho c^2 v_3^c = -\frac{\partial\Pi}{\partial v_3^c} = -p_{44}v_3^c$$

whose matrix form is

$$c^2\rho\mathbf{v}^c = \frac{\partial\Pi}{\partial\mathbf{v}^c} = -\mathcal{F}_s = \mathcal{E}\mathbf{v}^c. \tag{13}$$

With the purpose of relating the expression (13) with the velocities of the modes of propagation, we write

$$c^2\rho^{1/2}\mathbf{v}^c = \rho^{-1/2}\mathcal{E}\rho^{-1/2}\rho^{1/2}\mathbf{v}^c. \tag{14}$$

Defining $\overline{\mathbf{v}}^c = \rho^{1/2}\mathbf{v}^c$ and $\mathcal{S} = \rho^{-1/2}\mathcal{E}\rho^{-1/2}$, the equation (14) can be written as

$$c^2\overline{\mathbf{v}}^c = \mathcal{S}\,\overline{\mathbf{v}}^c. \tag{15}$$

The three positive wave speeds, $(c_i)_{1\le i\le 3}$, that verify (15) are solutions of

$$\det(\mathcal{S} - c^2 I) = 0.$$

Then, $c_1 = \sqrt{\dfrac{p_{33}}{\rho}}$, $c_2 = \sqrt{\dfrac{p_{55}}{\rho}}$ and $c_3 = \sqrt{\dfrac{p_{44}}{\rho}}$.

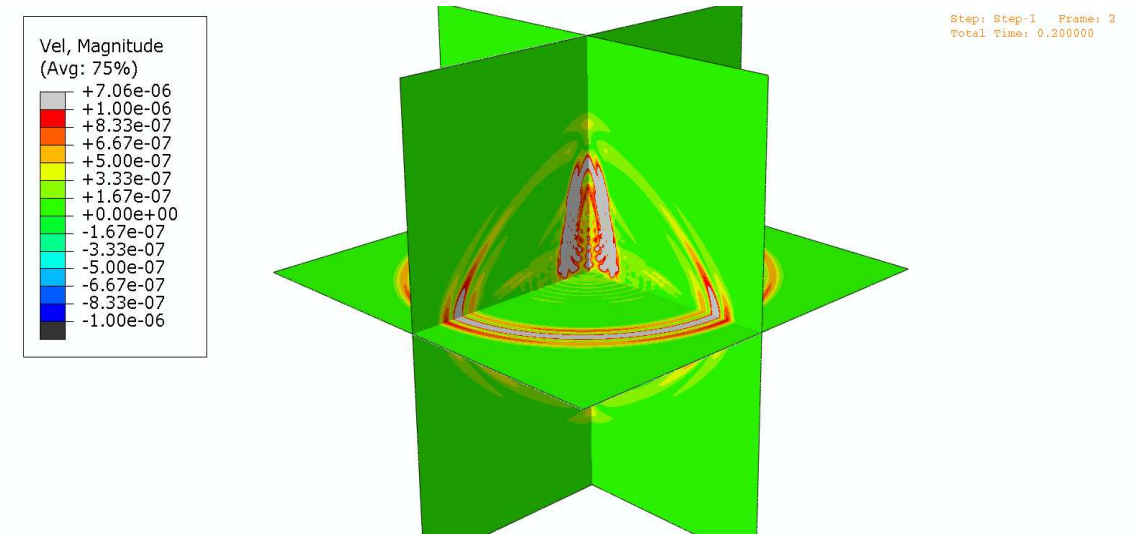

Figure 3: 3D VTI wave fronts. Snapshot of displacement magnitude at 200 ms.

The strain energy density on the surface Γ in terms of $\overline{\mathbf{v}}^c$ is

$$\overline{\Pi}(\overline{\mathbf{v}}^c) = \Pi(\mathbf{v}^c) = \frac{1}{2}(\mathbf{v}^c)^t \mathcal{S}\mathbf{v}^c$$
$$= \frac{1}{2}[\rho^{1/2}(\mathbf{v}^c)^t]\rho^{-1/2}\mathcal{S}\rho^{-1/2}(\rho^{1/2}\mathbf{v}^c) = \frac{1}{2}\overline{\mathbf{v}}^c\,\mathcal{S}\,\overline{\mathbf{v}}^c.$$

Finally, the first order absorbing boundary condition on Γ is of the form

$$-\mathcal{F}_s = -(\tau\nu\cdot\nu, -\tau\nu\cdot\chi^1, -\tau\nu\cdot\chi^2) = \mathcal{B}(\dot{\mathbf{u}}\cdot\nu, \dot{\mathbf{u}}\cdot\chi^1, \dot{\mathbf{u}}\cdot\chi^2), \tag{16}$$

being $\mathcal{B} = \rho\mathcal{S}^{1/2}$ positive definite. Therefore, the equation (16) allows to know the ABC given in (5).

4 RESULTS

To show the performance of the ABC we consider a Transversely Isotropic medium with Vertical symmetry axis (VTI). The curvature of the wavefronts are a measure of the degree of the anisotropy of the medium. The computational domain consists of a cube of side length 1500 m being its partition 200×200×200 cubic cells. The source is compressional and located at the center of the domain. Its central frequency is 30 Hz and the solution was computed for 160 frequencies in the range 0-80 Hz. The Figure 3 is a snapshot of the magnitude of the displacement at 200 ms. In correspondence with a VTI medium, qP and qSV waves propagate in vertical anisotropic planes. The qP-wavefront is traveling fastest and is highly attenuated in the vertical direction. A P-wavefront is propagating in the horizontal isotropic plane. The slow qSV-wavefront is clearly seen. At this time, no wave has arrived to the boundaries of the domain.

Snapshot of the magnitude of the displacement at 350 ms is shown in Figure 4. The behaviour of the ABC is illustrated for P-wavefront, no spurious reflections from the artificial boundaries are observed.

In the next simulation, the propagation of waves takes place in a Titled Transverse Isotropic (TTI) medium (VTI is rotated 30°). Figure 5 shows snapshots of the magnitude of the displacement at different times. We only focus what happens on the boundaries of the domain. At 233

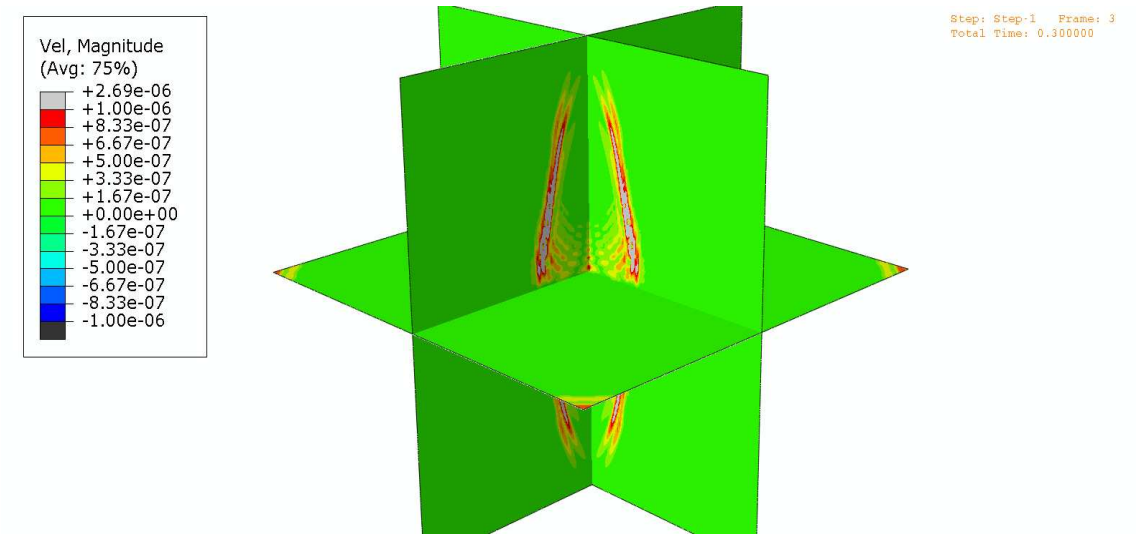

Figure 4: 3D VTI wave fronts. Snapshot of displacement magnitude at 350 ms to show how are working the ABC.

ms, the qP-wavefront is arriving to the boundaries of the domain. With the passage of time, at 266 ms and 300 ms, these boundaries behave like artificial boundaries by the application of the ABC.

The boundaries are also virtually transparent to the qSV-wavefronts that still have not arrived to them at the times of the figures.

5 CONCLUSION

We deduce a low-order ABC for the tridimensional wave equation. The equations for these ABC are derived from kinematic conditions, considering continuity of the displacements across the boundary, from dynamic conditions, using momentum equations of the wave fronts arriving normally to the boundary and expressions for the strain energy density along it.

We highlight that these ABC can be applied to any type of anisotropy and they are an alternative to the PMLs for three-dimensional wave propagation.

6 ACKNOWLEDGMENTS

This research was supported in part by Universidad Nacional de La Plata. The authors acknowledge the technical support of the Facultad de Informática, UNLP.

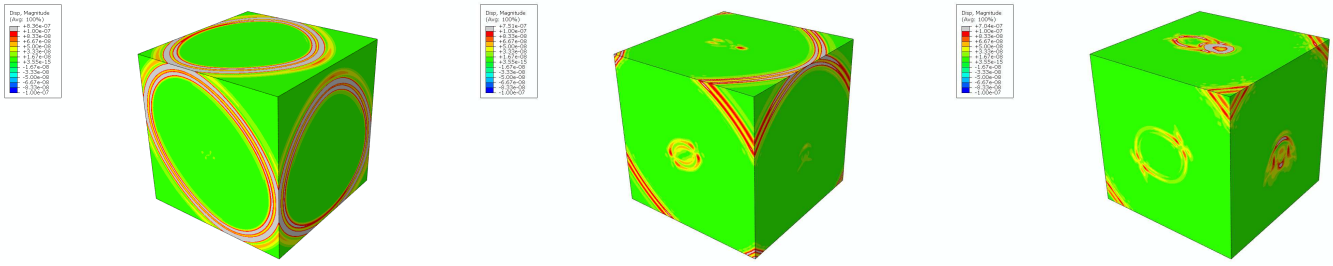

Figure 5: Displacement magnitude at different times in a TTI medium.

REFERENCES

Aki K. and Richards P. *Quantitative Seismology*. W.N. Freeman & Co., 1980.

Bécache E., Givoli D., and Hagstrom T. High-order absorbing boundary conditions for anisotropic and convective wave equations. *Journal of Computational Physics*, 229:1099–1129, 2010.

Bérenger J. A perfectly matched layer for the absorption of electromagnetic waves. *Journal of Computational Physics*, 114:185–200, 1994.

Boillot L., Barucq H., Diaz J., and Calandra H. Absorbing boundary conditions for 3d elastic tti modeling. In *SEG New Orleans Annual Meeting*, pages 535–540. DOI http://dx.doi.org/10.1190/segam2015-5910360.1, 2015.

Collino F. and Tsogka C. Finite element and finite volumes. two good friends. *Geophysics*, 66:294–307, 2001.

Engquist B. and Majda A. Finite element and finite volumes. two good friends. *Mathematical Computation*, 31:629–651, 1977.

Komatitsch D. and Tromp J. A perfectly matched layer absorbing boundary condition for the second-order seismic wave equation. *Geophysical Journal International*, 154:146–153, 2003.

Landau L. and Lifshitz E. *Theory of Elasticity. Course of Theoretical Physics*, volume 7. Pergamon, 1959.

Loeve A. *A Treatise on the Mathematical Theory of Elasticity*. Dover, New York, 1944.

Lovera O. and Santos J. Numerical methods for a model for wave propagation in composite anisotropic media. *Mathematical Modelling and Numerical Analysis*, 22:159–176, 1988.

Savadatti S. and Gudatti M. Accurate absorbing boundary conditions for anisotropic elastic media. *Journal of Computational Physics*, 231:7584–7607, 2012.